Simultaneous amplification and compression of picosecond optical pulses during Raman amplification in optical fibers

Clifford Headley III and Govind P. Agrawal

The Institute of Optics, University of Rochester, Rochester, New York 14627

Received March 4, 1993; revised manuscript received June 17, 1993

A novel technique that can lead to simultaneous amplification and compression of picosecond optical pulses is proposed. It consists of copropagating a weak signal pulse with an intense pump pulse in an optical fiber whose minimum-dispersion wavelength is chosen such that it falls between the pump and the signal wavelengths. The pump pulse amplifies the signal pulse through stimulated Raman scattering and at the same time imposes a nearly linear frequency chirp on it through cross-phase modulation. The chirped signal pulse is simultaneously compressed in the anomalous-dispersion regime of the optical fiber as it becomes amplified. Numerical simulations are used to predict the extent of amplification and compression under realistic practical conditions. The signal pulse can be compressed by more than a factor of 10 while it is amplified by 40–50 dB.

1. INTRODUCTION

An important application of stimulated Raman scattering (SRS) in optical fibers is for the amplification of a weak optical pulse (signal pulse) copropagating with an intense pump pulse.[1–5] Such a device, the so-called fiber-Raman amplifier, requires that the carrier-frequency difference between the pump and the signal pulses fall within the bandwidth of the Raman-gain spectrum. Typically fiber-Raman amplifiers are used to amplify weak optical pulses without regard to their pulse-width changes during amplification. Many applications in the fields of optical fiber communications and photonic switching require ultrashort (subpicosecond or femtosecond) optical pulses. Such pulses are often obtained by use of pulse-compression techniques. Since these techniques are difficult to implement for weak pulses, the use of cross-phase modulation (XPM) for weak-pulse compression[6–11] and for converting weak cw beams into ultrashort pulses[12,13] by launching them together with an intense pump pulse has been studied. In these schemes XPM imposes a nearly linear positive chirp (frequency increases with time) on the signal pulse. The pulse can be compressed or the cw beam pulsed by then passing through a dispersive medium with an anomalous group-velocity dispersion (GVD). When the wavelength of the signal pulse is in the anomalous-dispersion regime of the fiber, an all-fiber compression scheme can be used both to chirp and to compress the signal pulse.[6,12,13] The possibility of combining the fiber-Raman amplifier with an all-fiber compression scheme to achieve both amplification and compression of the signal pulse does not appear to have been studied so far.

Our objective in this paper is to study theoretically how one can use SRS in a single-mode optical fiber to amplify and compress a picosecond pulse simultaneously by launching it together with a pump pulse. The paper is organized as follows. In Section 2 coupled-amplitude wave equations that include the effects of SRS, XPM, self-phase modulation, and GVD are presented. The equations are then rewritten in a more convenient normalized form. In Section 3 the results of numerical simulations showing simultaneous pulse compression and amplification are presented and discussed for the case of equal pulse widths and group velocities for the pump and the signal pulses. In subsequent sections we relax these restrictions to study the practicality of this technique. In Section 4 we examine what happens when the pump power is varied, while in Section 5 we consider the effect of varying the ratio of the signal-pulse width to the pump-pulse width. In Section 6 the walk-off effects on the process resulting from the group-velocity mismatch are discussed. Finally, the results are summarized in Section 7.

2. THEORETICAL MODEL

A set of coupled amplitude equations describing the evolution of copropagating pump and signal pulses in an optical fiber that includes SRS, XPM, self-phase modulation, and GVD can be written as (in the notation of Ref. 3)

$$\frac{\partial A_p}{\partial z}+\frac{1}{v_{gp}}\frac{\partial A_p}{\partial t}+\frac{i}{2}\beta_{2p}\frac{\partial^2 A_p}{\partial t^2} = i\gamma_p(|A_p|^2+2|A_s|^2)A_p-\frac{g_p}{2}|A_s|^2A_p, \quad (1)$$

$$\frac{\partial A_s}{\partial z}+\frac{1}{v_{gs}}\frac{\partial A_s}{\partial t}+\frac{i}{2}\beta_{2s}\frac{\partial^2 A_s}{\partial t^2} = i\gamma_s(|A_s|^2+2|A_p|^2)A_s+\frac{g_s}{2}|A_p|^2A_s, \quad (2)$$

where $A_j(z,t)$ with $j=p$ or $j=s$ is the (complex) amplitude of the pulse envelope, v_{gj} is its group velocity, β_{2j} is the GVD coefficient, γ_j is the nonlinearity parameter, and g_j is the Raman-gain parameter. The parameter γ_j is related to the nonlinear-index coefficient n_2 by the expression $\gamma_j=2\pi n_2/(\lambda_j A_{\text{eff}})$, where A_{eff} is the effective core area of the fiber and λ_j is the wavelength of the pulse. The Raman-gain parameter g_j is related to the measured Raman-gain coefficient g_{Rj} (in meters per watt) by the expression $g_j=g_{Rj}/A_{\text{eff}}$. The first and second terms on the right-hand side of Eqs. (1) and (2) describe self-phase modulation and XPM, respectively.

0740-3224/93/122383-07$06.00

It is useful to write Eqs. (1) and (2) in a normalized form. To this end, the following dimensionless variables are introduced:

$$\tau = (t - z/v_{gp})/t_p, \qquad \xi = z|\beta_{2p}|/t_p^2,$$
$$U_p = A_p/\sqrt{P_0}, \qquad U_s = A_s/\sqrt{P_0}, \tag{3}$$

where t_p and P_0 set the time and the power scales, respectively, and are chosen as the pulse width and the peak power of the input pump pulse, respectively. Equations (1) and (2) then take the form

$$\frac{\partial U_p}{\partial \xi} + \text{sign}(\beta_{2p})\frac{i}{2}\frac{\partial^2 U_p}{\partial \tau^2} = iN^2(|U_p|^2 + 2|U_s|^2)U_p - \frac{qN^2}{2}|U_s|^2 U_p, \tag{4}$$

$$\frac{\partial U_s}{\partial \xi} - \delta\frac{\partial U_s}{\partial \tau} + \frac{i}{2}\frac{\beta_{2s}}{|\beta_{2p}|}\frac{\partial^2 U_s}{\partial \tau^2} = irN^2(|U_s|^2 + 2|U_p|^2)U_s + \frac{qrN^2}{2}|U_p|^2 U_s, \tag{5}$$

where $r = \lambda_p/\lambda_s$ is the ratio of the pump to the signal wavelengths. The parameter N is defined by

$$N^2 = \gamma_p P_0 t_p^2/|\beta_{2p}|. \tag{6}$$

N has physical significance in the anomalous-dispersion regime, where integer values of N correspond to fundamental and higher-order solitons. It is a useful parameter here in that it significantly reduces the number of variables in the problem. In an experimental situation, for a given piece of fiber and pump wavelength, the values of γ_p and β_{2p} are fixed. Furthermore, it is likely that the pump-pulse width available is fixed. Hence, from a practical standpoint N^2, as given in Eq. (6), can be considered a measure of the peak power of the pump pulse. The parameter q in the last terms of Eqs. (4) and (5) represents the ratio

$$q = \frac{g_p}{\gamma_p} = \frac{\lambda_p g_{Rp}}{2\pi n_2}. \tag{7}$$

The term $\lambda_p g_{Rp}$ is a constant given approximately by 1×10^{-19} m^2/W at the peak of the Raman-gain spectrum, and $n_2 = 3.2 \times 10^{-20}$ m^2/W for fused silica, yielding $q \approx 1/2$ for a frequency difference between the pump and the signal wave of ~13.2 THz; q becomes smaller when the frequency difference deviates from this value. We use $q = 1/2$ in our numerical simulations. Finally, in Eqs. (4) and (5)

$$\delta = t_p(v_{gp}^{-1} - v_{gs}^{-1})/|\beta_{2p}| \tag{8}$$

is a normalized walk-off parameter that accounts for the group-velocity mismatch between the two pulses.

Equations (4) and (5) are the basic propagation equations for the study of the Raman amplification of optical pulses. In Section 3 numerical solutions to these equations are presented. A fast-Fourier-transform-based split-step method is used.[3] The input pump and signal pulses are assumed to be Gaussian in shape, and the Raman gain is assumed to be constant across the spectral width of the pump and the signal waves. The complex amplitude

$$U_s(\xi,\tau) = |U_s(\xi,\tau)|\exp[i\phi(\xi,\tau)]$$

of the signal pulse after it propagates a distance ξ is used to obtain the pulse shape governed by the intensity profile $|U_s(\xi,\tau)|^2$ and the frequency chirp, defined as $\Delta\nu_c = -\partial\phi/2\pi\partial\tau$. We obtain signal spectrum $|\tilde{U}_s(\xi,\nu)|^2$ by taking the Fourier transform of $U_s(\xi,\nu)$ according to the relation

$$\tilde{U}_s(\xi,\nu - \nu_0) = \int U_s(\xi,\tau)\exp[i(\nu - \nu_0)\tau]d\nu, \tag{9}$$

where $\nu_0 = c/\lambda_s$ is the carrier frequency of the signal pulse.

3. RAMAN AMPLIFICATION AND COMPRESSION

To demonstrate the potential of the proposed Raman-amplification scheme, we first consider the case in which pump and signal pulses of equal widths are incident at the input end of an optical fiber whose minimum-dispersion wavelength λ_D is chosen such that it lies exactly in the center between the pump and the signal wavelengths, i.e., $\lambda_s - \lambda_D = \lambda_D - \lambda_p$. This approach is similar to that taken by several authors.[4,5,12,13] As a specific example, 1.55-μm picosecond pulses emitted from a mode-locked erbium-doped fiber laser can be amplified by being copropagated with 1.45-μm pump pulses (obtained from a color-center laser, for example) in a dispersion-shifted fiber such that $\lambda_D \approx 1.5$ μm. Under such conditions both pulses travel at the same speed, and the walk-off parameter δ in Eq. (8) can be set to zero. Furthermore, $\beta_{2s} \approx -\beta_{2p}$ as long as the GVD varies approximately linearly with the wavelength in the vicinity of λ_D. The GVD curve for such a fiber is illustrated schematically by the diagonal solid line in Fig. 1, which shows the GVD as a function of

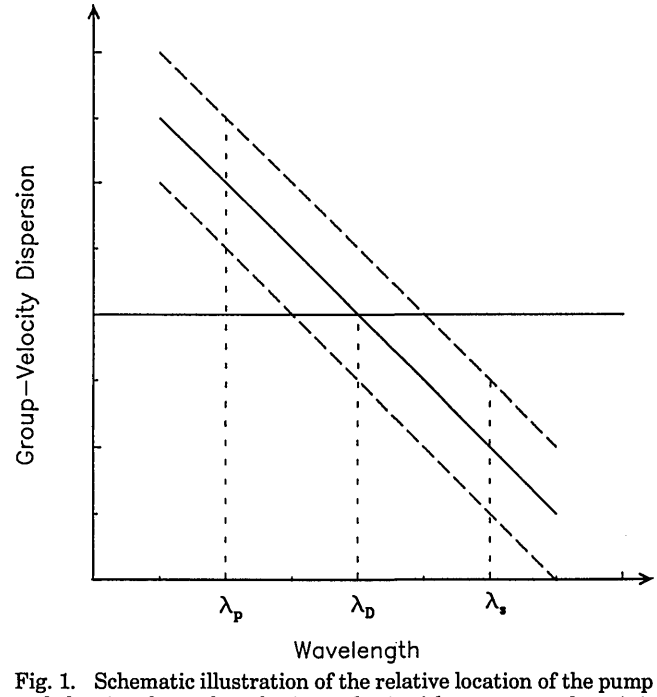

Fig. 1. Schematic illustration of the relative location of the pump and the signal wavelengths (λ_p and λ_s) with respect to the minimum dispersion wavelength of the fiber, λ_D. The diagonal solid line shows the case in which λ_D is exactly in the center so that $v_{gp} = v_{gs}$ and $\beta_{2s} = -\beta_{2p}$. The diagonal dashed lines show how β_{2s} and β_{2p} change when λ_D shifts so that the group velocities of the pump and signal pulses are not equal.

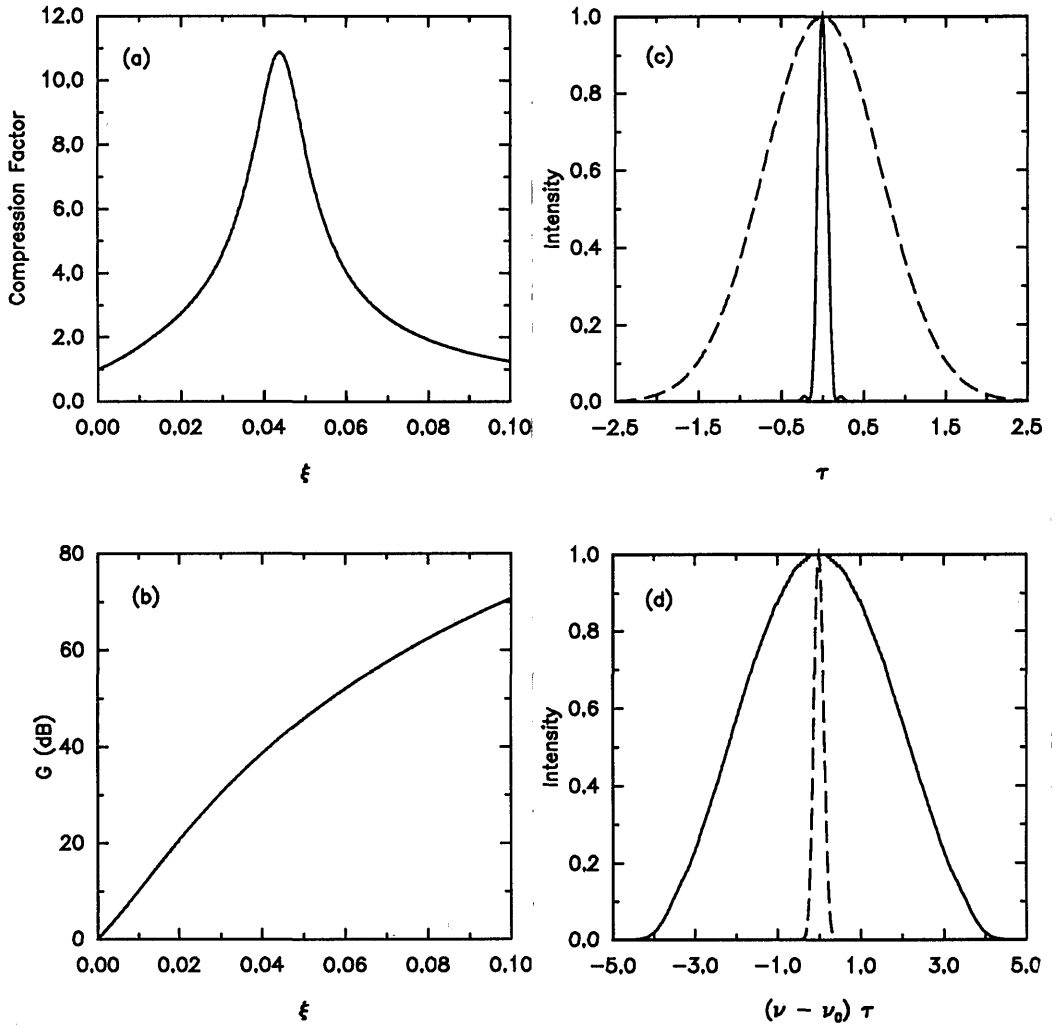

Fig. 2. Compression factor, amplification factor, pulse shape, and pulse spectrum of signal pulse for $N = 25$, equal pulse widths ($t_s = t_p$), and equal group velocities ($\delta = 0$). (a) Compression factor as a function of normalized distance ξ. (b) Amplification factor as a function of normalized distance ξ. (c) Pulse shape as a function of normalized retarded time τ and (d) pulse spectrum as a function of normalized shifted frequency $(\nu - \nu_0)\tau$ at $\xi = 0.0438$, the distance at which maximum compression occurs. In (c) and (d) the input pulse shape and spectrum are shown for comparison by a dashed curve.

wavelength. The absence of walk-off maximizes both XPM interaction and Raman amplification, since the two pulses continue to overlap throughout the fiber. For this choice of wavelengths $r = 0.94$. We choose $N = 25$. Using the typical values $\gamma_p = 3\ \mathrm{km^{-1}\,W^{-1}}$, $|\beta_{2p}| = 5\ \mathrm{ps^2/km}$, and $t_p = 10$ ps, this value of N corresponds to an input pump peak power of ~10 W. Such peak powers can be obtained even from semiconductor lasers operating at a 100-MHz repetition rate with 10–20 mW of average power.

Two parameters are used to quantify the amount of compression and amplification experienced by a pulse. The compression factor X is defined as

$$X(\xi) = \sigma(0)/\sigma(\xi), \tag{10}$$

where rms width $\sigma(\xi)$ of a pulse at the distance ξ is defined by

$$\sigma^2 = \langle \tau^2 \rangle - \langle \tau \rangle^2, \tag{11}$$

with

$$\langle \tau^m \rangle = \frac{\int_{-\infty}^{\infty} \tau^m |U_s(\xi,\tau)|^2 d\tau}{\int_{-\infty}^{\infty} |U_s(\xi,\tau)|^2 d\tau}. \tag{12}$$

The energy amplification factor G is defined as

$$G(\xi) = \frac{\int_{-\infty}^{\infty} |U_s(\xi,\tau)|^2 d\tau}{\int_{-\infty}^{\infty} |U_s(0,\tau)|^2 d\tau}. \tag{13}$$

Figures 2(a) and 2(b) show the variation of the compression factor $X(\xi)$ and the amplification factor $G(\xi)$ with the normalized distance ξ. Figure 2(a) shows that at a distance of $\xi = 0.0438$ (actual fiber length using simulation parameters, ≈0.88 km) the signal pulse is compressed by a factor of 11. At this same distance, Fig. 2(b) shows that the signal pulse has been amplified by ~40 dB. Figures 2(c) and 2(d) show the pulse shape and spectrum of

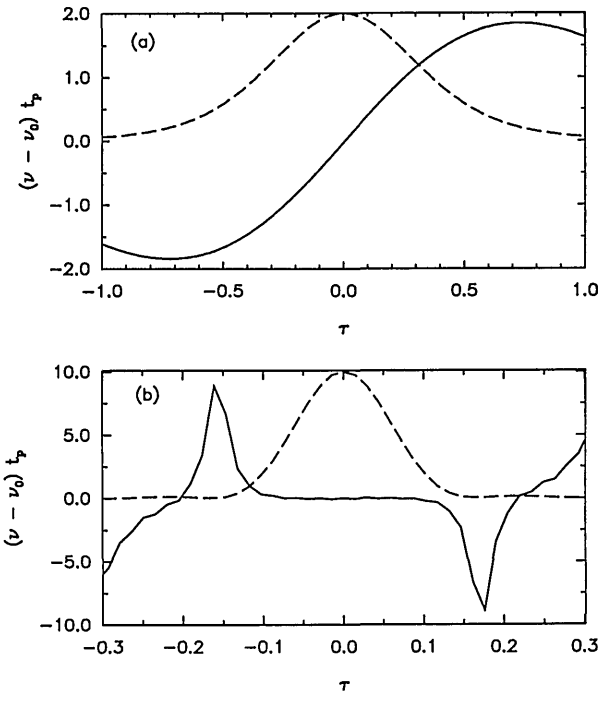

Fig. 3. Signal-pulse chirp (solid curve) under conditions identical to Fig. 1 at (a) $\xi = 0.02$ and (b) $\xi = 0.0438$, the normalized distance at which maximum compression occurs. The pulse shapes (dashed curve) at the corresponding distances are also shown for comparison.

the signal pulse at the input of the fiber (dashed curve) as well as at the distance where maximum compression occurs (solid curve).

The amplification of the signal pulse is clearly occurring through SRS. Figure 3, which shows the chirp on the signal pulse at [Fig. 3(a)] $\xi = 0.0200$ and [Fig. 3(b)] $\xi = 0.0438$ (distances before and at maximum compression), illustrates the process by which pulse compression occurs.[8] The dashed curves in Fig. 3 represent the corresponding pulse shapes. Initially, nonlinear effects dominate and XPM imposes a positive chirp on the signal pulse [Fig. 3(a)]. Since the signal pulse is traveling in the anomalous-dispersion regime (red-frequency components travel slower than blue components), the trailing edge attempts to catch up with the leading edge, and the pulse is compressed. At the point of maximum compression dispersion has reduced the chirp to nearly zero across the pulse [Fig. 3(b)]. A weak oscillatory structure seen in Fig. 2(c) around the base of the pulse results from the chirp's not being linear in the pulse wings.

Since we have seen that under certain conditions it is possible to produce chirp-free amplified and compressed pulses, the robustness of this scheme must be studied when the assumptions made are relaxed. Over the next few sections the effect on the process of changing the pump power and the pulse-width ratios and of introducing a group-velocity mismatch are explored.

4. EFFECT OF PUMP POWER ON RAMAN AMPLIFICATION AND PULSE COMPRESSION

As is discussed above, one can study the effects of varying the pump power by changing the parameter N [see Eq. (6)]. The calculated results for values of $N = 10$, 20, 30, and 40 are presented in Fig. 4. Figure 4(a) shows the compression factor X as a function of ξ, and Fig. 4(b) the amplification factor G. Both X and G increase with increasing pump power, but the distance at which maximum compression occurs decreases. There is no significant change in pulse quality for all values of N in the range 10–40.

The behavior seen in Fig. 4 can be easily understood. When GVD is negligible, the maximum chirp $\Delta\nu_{\max}$ initially experienced by the signal pulse through XPM can be written as[7,14]

$$\Delta\nu_{\max} = \frac{\gamma_s P_0 t_p}{\pi|\delta\beta_{2p}|}. \tag{14}$$

A larger pump power (or larger N) leads to a larger chirp bandwidth[7,14,15] across the signal pulse and a broader signal-pulse spectrum. At the point of maximum compression, where the chirp is zero, the broader spectrum yields a narrower signal pulse in the time domain, resulting in more compression. The results in Fig. 4 show a compression by a factor of 15 for $N = 40$. However, higher compression factors can be obtained for larger values of N simply because the XPM-induced chirp increases.[4,15] XPM is known to produce compression factors as high as ~50 for $N > 20$.[12] The increased chirp bandwidth that accompanies increased pump power also explains the decreased distance over which maximum compression occurs. As the frequency difference between the leading and the trailing edges of the pulse increases, the distance needed for the wings to be compressed decreases. The increase in the amplification factor of the signal pulse at the distance for which maximum compression occurs implies that the increase in pump power is sufficient to compensate for the decreased distance over which the pulses interact.

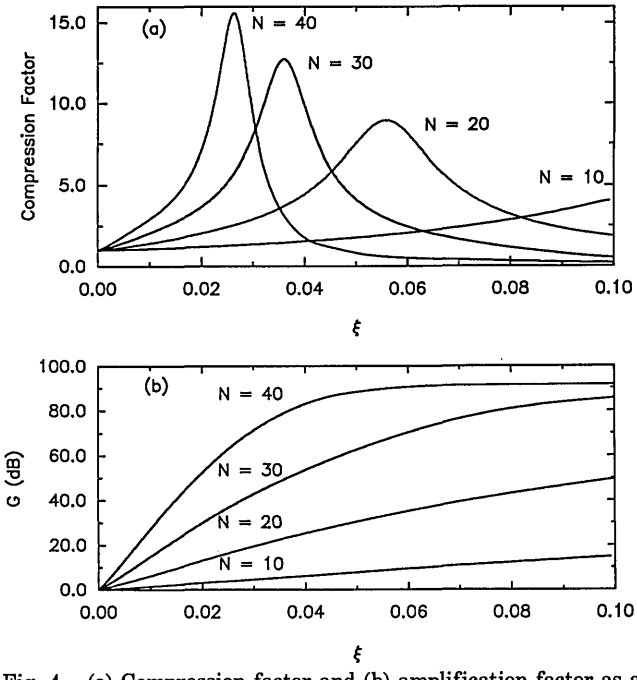

Fig. 4. (a) Compression factor and (b) amplification factor as a function of normalized distance ξ for several values of N with $t_s = t_p$ and $\delta = 0$.

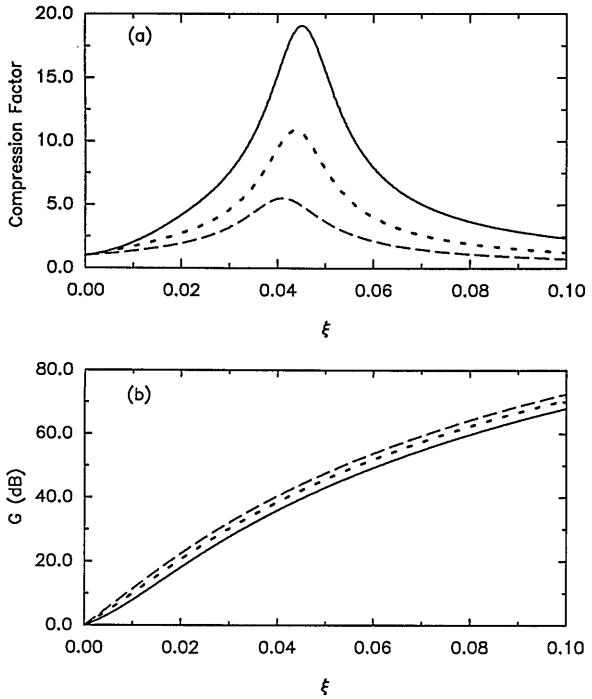

Fig. 5. (a) Compression factor and (b) amplification factor as a function of normalized distance ξ for $N = 25$ and $\delta = 0$ with $t_s/t_p = 2$ (solid curve), $t_s/t_p = 1$ (dotted curve), and $t_s/t_p = 0.5$ (dashed curve).

The conclusion here is that this technique can be used for a broad range of pump-pulse powers. As the pump power is increased, more amplification and compression are obtained for a shorter piece of fiber.

5. PUMP AND SIGNAL PULSES OF UNEQUAL WIDTHS

In experimental circumstances it may prove difficult to match the pulse widths of the pump and the signal wavelengths exactly. In this section the effect of unequal pulse widths is examined. Figure 5 shows the results of varying the signal-to-pump pulse-width ratio, t_s/t_p, from 0.5 to 2 by variation of the signal pulse width for $N = 25$. Figure 5(a), a plot of the compression factor as a function of ξ, shows that the amount of compression increases as the pulse-width ratio increases. There is, however, a slight decrease in the amplification of the signal pulse with an increasing pulse-width ratio, and this is shown in Fig. 5(b), which is a plot of the amplification factor versus distance. Figures 6(a) and 6(b) show the signal pulse at the distance of maximum compression for pulse-width ratios of 2 and 0.5, respectively. These can be compared with Fig. 2(c). It is seen that the quality of the compressed pulse changes with the pulse-width ratio.

The increase in the compression factor and the change in pulse quality can be explained as follows.[8,15] Figure 3(a) shows that the chirp impressed on the signal pulse by the pump pulse is nearly linear only over the central portion of the signal pulse. When the signal pulse is much narrower than the pump pulse, the chirp imposed on the signal pulse is nearly linear across most of the pulse, and hence the absence of oscillatory structure in Fig. 6(b). As the ratio t_s/t_p is increased, the chirp bandwidth across the signal pulse also increases, leading to more compression. However, an increasingly larger portion of the signal-pulse wings obtain a nonlinear chirp, which leads to an oscillatory structure in the wings of the pulse [Fig. 2(c)]. Eventually, as the signal pulse becomes wider than the pump pulse, only the central portion of the signal pulse can be compressed [Fig. 6(a)]. These results agree with previous results, which show that the effect of XPM is reduced when the pulse-width ratio decreases.[15] The increase in amplification of narrow signal pulses occurs simply because these pulses are amplified by only the central, more intense portion of the pump pulse. However, since the distance at which the maximum compression occurs also decreases with a decreasing pulse-width ratio, there is little change in the amplification of the pulse at the point of maximum compression. The decrease in distance at which maximum compression occurs as the pulse-width ratio decreases can be explained as follows. As is explained in Section 3, pulse compression is occurring through the competing chirps from XPM and GVD. Eventually GVD will dominate, and the pulse will begin to broaden. This happens for two reasons. First, the pump weakens because of linear and nonlinear loss. The second and more important reason is that the chirp introduced by GVD per unit propagation length increases with an increasing spectral width of the pulses. With the chirp from XPM connected to a broadening of the spectral width, it is clear that GVD will dominate at some point. It follows that the shorter the pulse is from the start, the broader the spectrum and the smaller the XPM chirp (for a given pump), hence the shorter the distance needed for GVD to dominate.

The conclusion is that, as the signal pulse width is increased for a given pump pulse, more compression can be

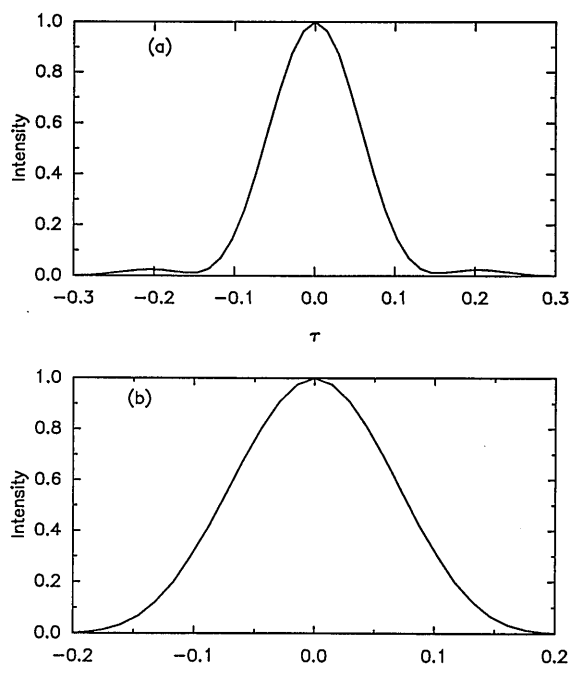

Fig. 6. Normalized signal-pulse intensity for $N = 25$ and $\delta = 0$. (a) $t_s/t_p = 2$; $\xi = 0.0451$, the normalized distance at which maximum compression occurs. (b) $t_s/t_p = 0.5$; $\xi = 0.0412$, the normalized distance at which maximum compression occurs.

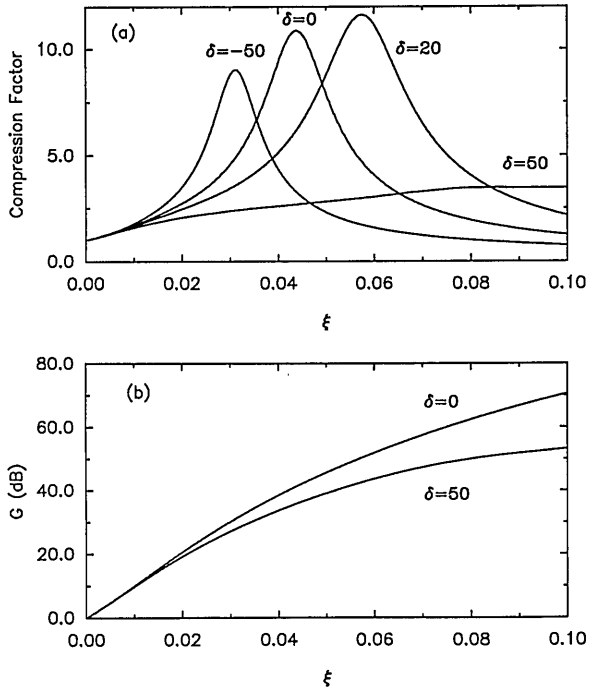

Fig. 7. (a) Compression factor and (b) amplification factor as a function of normalized distance ξ for several values of the walk-off parameter δ when $N = 25$ and $t_s = t_p$.

obtained, with little change in the amplification factor of the pulse. However, the quality of the compressed pulse is not so good as for broader signal pulses.

6. EFFECT OF GROUP-VELOCITY MISMATCH

Thus far it has been assumed that there is no walk-off between the pump and the signal pulses, something difficult to realize in practice. In this section the effect of walk-off is studied. For a fiber whose GVD near the minimum-dispersion wavelength is given by Fig. 1, the presence of a group-velocity mismatch implies that the wavelength at which minimum dispersion occurs is no longer centered between the pump and the signal wavelengths. This is illustrated in Fig. 1 by the two dashed diagonal lines. Hence the effect of walk-off is to change not only the value of δ but also the ratio $\beta_{2s}/|\beta_{2p}|$ in Eq. (5).

Figure 7(a) shows the compression factor for values of $\delta = -50$, 0, 20, 50, and Fig. 7(b) the amplification factor for $\delta = 0$, 50. For values of $\delta = -50$ and $\delta = 20$ the amplification factor was slightly less, but not significantly different from that for $\delta = 0$. With the simulation parameters outlined in Section 3, the values of $\delta = -50$, 20, 50 correspond to shifts in the minimum-dispersion wavelength of the fiber of 13.5 nm, −9 nm, and −30 nm, respectively. Figure 7(a) shows that the proposed scheme works well even in the presence of group-velocity mismatch for δ in the range from −50 to 20. Figure 8 shows the signal pulse for $\delta = -50$ and $\delta = 20$ in the reference frame in which the pump pulse is centered at $\tau = 0$. The signal pulse walks off because of group-velocity mismatch but remains contained within the pump pulse mainly because it becomes compressed. There is no significant change in the quality of the compressed pulses compared with the case $\delta = 0$ shown in Fig. 2(c).

It is useful to consider what happens as the minimum-dispersion wavelength of the fiber is shifted between λ_p and λ_s. As δ is increased, the minimum-dispersion wavelength shifts toward the signal wavelength, and $|\beta_{2p}|$ increases while $|\beta_{2s}|$ decreases. Clearly, when $\lambda_D > \lambda_s$, the scheme will no longer work, since it is necessary for the signal wavelength to be in the anomalous-dispersion regime of the fiber for pulse compression to occur. The curves for $\delta = 50$ in Fig. 7(a) and 7(b) show that the signal pulse is still being compressed and amplified when λ_D has been shifted such that $\lambda_D - \lambda_p = 0.8(\lambda_s - \lambda_p)$. On the other hand, when δ is decreased and the minimum-dispersion wavelength of the fiber approaches the pump wavelength, $|\beta_{2p}|$ decreases and $|\beta_{2s}|$ increases. The scheme will work, albeit with less compression and amplification. When $\lambda_D < \lambda_p$, the pump pulse is also traveling in the anomalous-dispersion regime of the fiber. The pump pulse then behaves as a higher-order soliton and may itself experience compression.[3] There is an increase in the compression factor when δ is changed from 0 to 20. This may imply that a slight walk-off in beneficial to the compression process. In reality walk-off is never beneficial, since it reduces the chirp from XPM.[9,13] The increased compression is due to N's being held constant at 25. Since $|\beta_{2p}|$ has increased, Eq. (6) implies that N should be reduced at a constant power. By holding N constant, it is assumed that pump power is increased to compensate for the increase in pump GVD. This increased power accounts for the increased compression seen in Fig. 7(a) as δ is varied from 0 to 20.

The increase in the distance at which maximum compression occurs as δ is changed from −50 to 20 is due to the decrease in $|\beta_{2s}|$. Since the GVD describes the rate at which the frequency components of the chirped pulse come together, a smaller value implies that a longer length of fiber is necessary for compression to take place. The

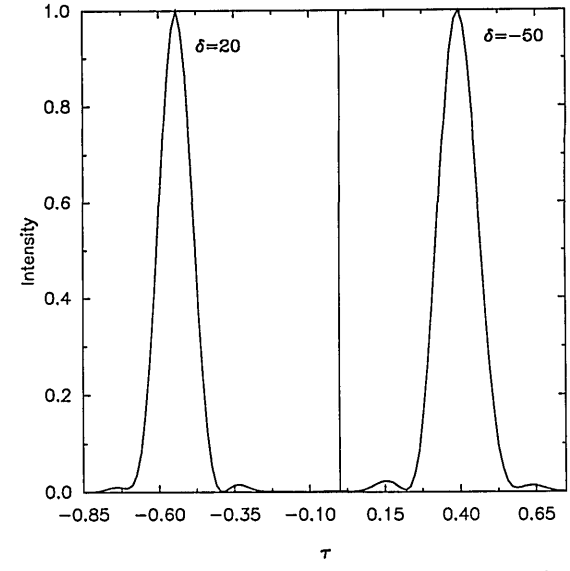

Fig. 8. Normalized signal-pulse intensity for $N = 25$ and $t_s = t_p$ with $\delta = 20$ and $\delta = -50$ at the distances where maximum compression occurs. The pump pulse is centered at the normalized retarded time $\tau = 0$. The signal pulse moves away from the pump pulse owing to the group-velocity mismatch.

increased length of fiber necessary for maximum compression to occur as δ is increased implies that the amplification factor also increases when δ is varied between -50 and 20.

The conclusion here is that the proposed scheme is quite forgiving to small group-velocity mismatches at the pump and the signal wavelengths.

7. CONCLUSIONS

In this paper a technique is proposed for using SRS in a fiber to amplify and compress a weak signal pulse simultaneously by copropagating it with a more intense pump pulse. Numerical simulations are used to predict the extent of pulse compression and the corresponding amplification factor. Particular attention is paid to the case of equal pulse widths and group velocities of the pump and the signal pulses. Increasing the pump power leads to improved compression and amplification without a significant change in the quality of the pulse. The scheme works reasonably well when there is a mismatch between the pump and the signal pulse widths. The amplification of the pulse remains fairly constant, while the compression factor increases with increasing signal pulse width at the expense of pulse quality. Finally, it is shown that the technique remains applicable for a small walk-off between the pulses. This scheme is particularly suited for the case in which 1.55-μm pulses obtained from semiconductor lasers or erbium-doped fiber lasers are simultaneously compressed and amplified by use of a dispersion-shifted fiber with minimum dispersion near 1.5 μm. The requirements for peak power of the 1.45-μm pump pulse are relatively modest (10 W of 10-ps pump pulse). It may even be possible to obtain such pulses from semiconductor lasers operating with 10–20-mW average power.

ACKNOWLEDGMENTS

The research reported here is supported by the U.S. Army Research Office, the National Science Foundation (grant ECS-9010599), and the New York State Center for Applied Optical Technology.

REFERENCES

1. C. Lin and R. H. Stolen, "Backward Raman amplification and pulse steepening in silica fibers," Appl. Phys. Lett. **29,** 428–431 (1976).
2. L. F. Mollenauer, R. H. Stolen, and M. N. Islam, "Experimental demonstration of soliton propagation in long fibers: loss compensated by Raman gain," Opt. Lett. **10,** 229–231 (1985).
3. G. P. Agrawal, *Nonlinear Fiber Optics* (Academic, San Diego, 1989), Chap. 8.
4. A. S. Gouveia-Neto, A. S. L. Gomes, J. R. Taylor, and K. J. Blow, "Soliton reconstruction through synchronous amplification," J. Opt. Soc. Am. B **5,** 799–803 (1988).
5. A. S. Gouveia-Neto, P. G. J. Wigley, and J. R. Taylor, "Soliton generation through Raman amplification of pulses with subfundamental soliton powers," Opt. Commun. **72,** 119–122 (1989).
6. B. Jaskorzynska and D. Schadt, "All-fiber distributed compression of weak pulses in the regime of negative group-velocity dispersion," IEEE J. Quantum Electron. **24,** 2117–2120 (1988).
7. G. P. Agrawal, P. L. Baldeck, and R. R. Alfano, "Optical wave breaking and pulse compression due to cross-phase modulation in optical fibers," Opt. Lett. **14,** 137–139 (1989).
8. G. P. Agrawal, P. L. Baldeck, and R. R. Alfano, "Temporal and spectral effects of cross-phase modulation on copropagating ultrashort pulses in optical fibers," Phys. Rev. A **40,** 5063–5072 (1989).
9. D. Schadt, B. Jaskorzynska, and U. Österberg, "Numerical study on combined stimulated scattering and self-phase modulation in optical fibers influenced by walk-off between pump and Stokes pulse," J. Opt. Soc. Am. B **3,** 1257–1262 (1986).
10. A. M. Weiner, J. P. Heritage, and R. H. Stolen, "Self-phase modulation and optical pulse compression influenced by stimulated Raman scattering in fibers," J. Opt. Soc. Am. B **5,** 364–372 (1988).
11. P. L. Baldeck, P. P. Ho, and R. R. Alfano, "Cross-phase modulation: a new technique for controlling the spectral, temporal, and spatial properties of ultrashort pulses," in *The Supercontinuum Laser Source*, R. R. Alfano, ed. (Springer-Verlag, New York, 1989), Chap. 4.
12. D. Schadt and B. Jaskorzynska, "Generation of short pulses from cw light by influence of crossphase modulation (cpm) in optical fibres," Electron. Lett. **23,** 1090–1091 (1987).
13. V. L. da Silva and C. H. Brito-Cruz, "Walk-off effect on the generation of ultrashort pulses from cw light using cross-phase modulation in optical fibers," J. Opt. Soc. Am. B **7,** 750–753 (1990).
14. P. L. Baldeck, R. R. Alfano, and G. P. Agrawal, "Induced frequency shift of copropagating ultrafast optical pulses," Appl. Phys. Lett. **52,** 1939–1941 (1988).
15. M. N. Islam, L. F. Mollenauer, R. H. Stolen, J. R. Simpson, and H. T. Shang, "Cross-phase modulation in optical fibers," Opt. Lett. **12,** 625–627 (1987).